Communication: Molecular Oxygen Generation from the Reaction of Water Cations with Oxygen Atoms

Ryan C. Fortenberry,[1,*] Tarek Trabelsi,[2] Brent R. Westbrook,[3] Weston A. Del Rio,[4] and Joseph S. Francisco[2]

[1]*Department of Chemistry & Biochemistry, University of Mississippi, University, Mississippi 38677-1848, U.S.A.; r410@olemiss.edu*

[2]*Department of Earth and Environmental Science Philadelphia, University of Pennsylvania, PA 19104, USA*

[3]*St. Edward's University, Department of Chemistry, Austin, TX 78704, USA*

[4]*Department of Chemistry & Biochemistry, University of Mississippi, University, Mississippi 38677-1848, U.S.A.*

(Dated: June 21, 2019)

Abstract

The oxywater cation (H_2OO^+), previously shown to form barrierlessly in the gas phase from water cations and atomic oxygen, is proposed here potentially to possess a $^2A'' \leftarrow {}^4A''$ excitation leading to the $H_2 \cdots O_2{}^+$ complex. This complex could then easily decompose into molecular hydrogen and the molecular oxygen cation. The present quantum chemical study shows that the necessary electronic transition takes place in the range of 1.92 eV (645 nm), in the orange-red range of the visible and solar spectrum, and dissociation of the complex only requires 5.8 kcal/mol (0.25 eV). Such a process for the abiotic, gas phase formation of O_2 would only need to be photocatalyzed by visible wavelength photons. Hence, such a process could produce O_2 at the mesosphere/stratosphere boundary as climate change is driving more water into the upper atmosphere, in the comet 67P/Churyumov-Gerasimenko where surprisingly high levels of O_2 have been observed, or at gas-surface (ice) interfaces.

Recent work has shown that, in the gas phase, water will form bonds originating on the oxygen atom with every atomic cation from hydrogen even to argon[1]. Quintessentially, hydronium (H_3O^+) is a pillar of acid-base chemistry and has even been observed in the interstellar medium (ISM)[2]. More interesting, though, the bonding of water cation with atomic oxygen is shown to be stable in forming the oxywater cation. In this molecule, the O−O bond energy is 54.08 kcal/mol[1] which is notably greater than that of hydrogen peroxide with a O−O bond energy of a meager 33.9 kcal/mol which is enough to be cleaved by sunlight. However, this present work will discuss a previously unreported quarternary minimum.

FIG. 1. The CCSD(T)-F12/cc-pVTZ-F12 one-dimensional potential energy surface (in kcal/mol) for the O−O stretch of H_2OO^+. Curves: cyan, $^1A'$ H_2OO; magenta, $X\ ^2A'$ H_2OO^+; red, $1\ ^2A''$ H_2OO^+; green, $1\ ^4A''$ H_2OO^+; and blue, $^2A''$ $H_2\cdots O_2{}^+$.

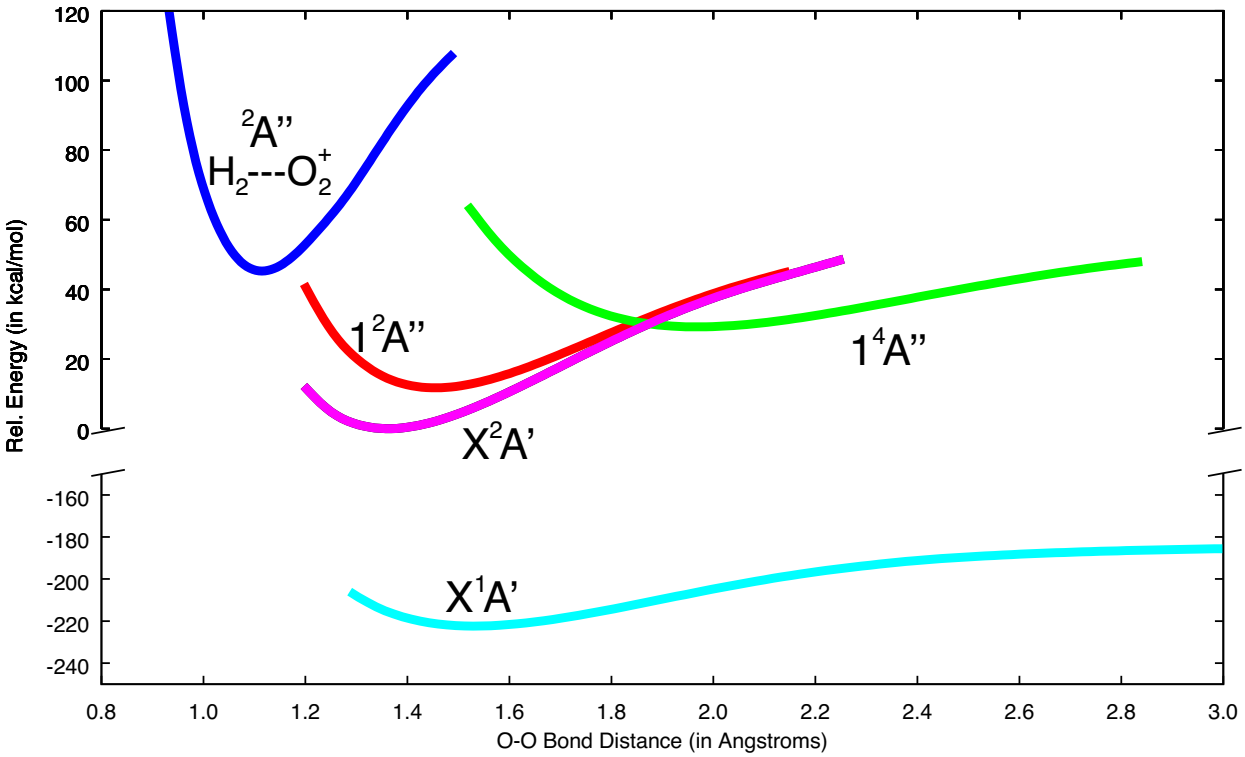

The creation of the oxywater cation (H_2OO^+)[3–5] from water cations and atomic oxygen progresses barrierlessly through a wide minimum for the association of O(^3P) to H_2O^+ potential energy surface (PES), shown in the green ($1\ ^4A''$) line of Figure 1 and previously demonstrated by Ref. 1. Then, electronic emission can create the doublet surface(s) (ma-

genta $X\ ^2A'$ and red $1\ ^2A''$ lines of Figure 1) where the molecule can relax into its optimized and stable minimum. In such a process, the resulting vibrational cascade would be reduced since the doublet surface crosses the quartet surface nearly at its minimum making the bonding reaction much faster than is typical of radiative association reactions which are notoriously slow. Consequently, these CCSD(T)-F12/cc-pVTZ-F12 computations[6,7] show that not only is the oxywater cation stable, but it should also form relatively easily[1]. These computations have also been verified with MRCISD(+Q)/aug-cc-pVTZ computations[8,9] giving the same potential energy curves as provided in Figure S1 of the supplemental information. Furthermore, these MRCI computations clearly show that formation of H_2OO^+ in this process likely is initiated with H_2O^+ and oxygen atoms. Formation through the alternate $O^+(^3S)$ and H_2O channel does not appear to couple with these low-lying states. Further work will explore this pathway.

The oxywater neutral will break apart more easily since the O−O bond dissociation energy is on the order of 40 kcal/mol (cyan $X\ ^1A'$ line in Figure 1). The ionization potential of H_2OO is computed here to be 9.58 eV, significantly more than the O−O bond energy as observed in Figure 1 where the magenta $X\ ^2A'$ line is well above the cyan $X\ ^1A'$ asymptotic dissociation limit. Futhermore, there do not appear to be any other states that interact with ground state of H_2OO. The oxywater cation, on the other hand, is more likely to engage in novel chemistry. Most notably, H_2OO^+ has another state of interest that gives many indications of leading to molecular oxygen.

The blue line in Figure 1 represents a $^2A''$ electronically excited state of a H_2OO^+ that ultimately gives rise to the $H_2\cdots O_2{}^+$ complex, H_2 weakly bound to $O_2{}^+$. The ionization potential of O_2 is notably less than H_2 (12.07 eV versus 15.43 eV)[10] likely forbidding the formation of the $O_2\cdots H_2{}^+$ system. Present CCSD(T)-F12/cc-pVTZ-F12 computations predict the optimized O−O bond length in this molecular complex to be 1.117 Å which is nearly exactly that for $O_2{}^+$ at 1.116 Å from experiment[10], putting the positive charge on the oxygen molecule portion. Additionally, with X defined as the center-of-mass in the H_2 portion, the optimized X−H value is 0.374 Å making H−H 0.748 Å, close to the experimental 0.741 Å for H_2[10]. The rest of the geometric parameters for $H_2\cdots O_2{}^+$, as well as the doublet and quartet forms of H_2OO^+ for comparison, are given in Table I.

The $^2A''$ $H_2\cdots O_2{}^+$ complex lies adiabatically 39.3 kcal/mol (1.70 eV) above the $X\ ^2A'$ ground state of H_2OO^+ and only a mere 12.6 kcal/mol (0.54 eV) above the $1\ ^4A''$ state. The

TABLE I. The CCSD(T)-F12/cc-pVTZ-F12 Optimized Geometries.[a]

	$X\ ^2A'$ H_2OO^+	$1\ ^4A''$ H_2OO^+	$^2A''$ $H_2\cdots O_2^+$
O−O (Å)	1.362	1.964	1.117
X−H (Å)	0.846	0.791	0.374
O−X (Å)	0.507	0.578	2.424
∠O−O−X (°)	137.4	112.9	111.5

[a]X represents the center-of-mass in the H_2 moiety, i.e. half of the H−H bond length. This parameter gives more generic coordinates between the two isomers.

binding of the oxygen molecular cation to the hydrogen molecule in $H_2\cdots O_2^+$ is computed here to be 5.8 kcal/mol from a simple products minus reactants model. While the O−X distance gives a fairly flat potential, the the ∠O−O−X angle is more rigid at the optimized 111.5° similar to ligands of NO^+[11].

FIG. 2. The H_2OO^+ MOs: a) $2a''$ HOMO-1, b) $7a'$ HOMO, c) $8a'$ LUMO; as well as the $H_2\cdots O_2^+$ MOs: d) $7a'$ HOMO-1, e) $2a''$ HOMO, f) $8a'$ LUMO.

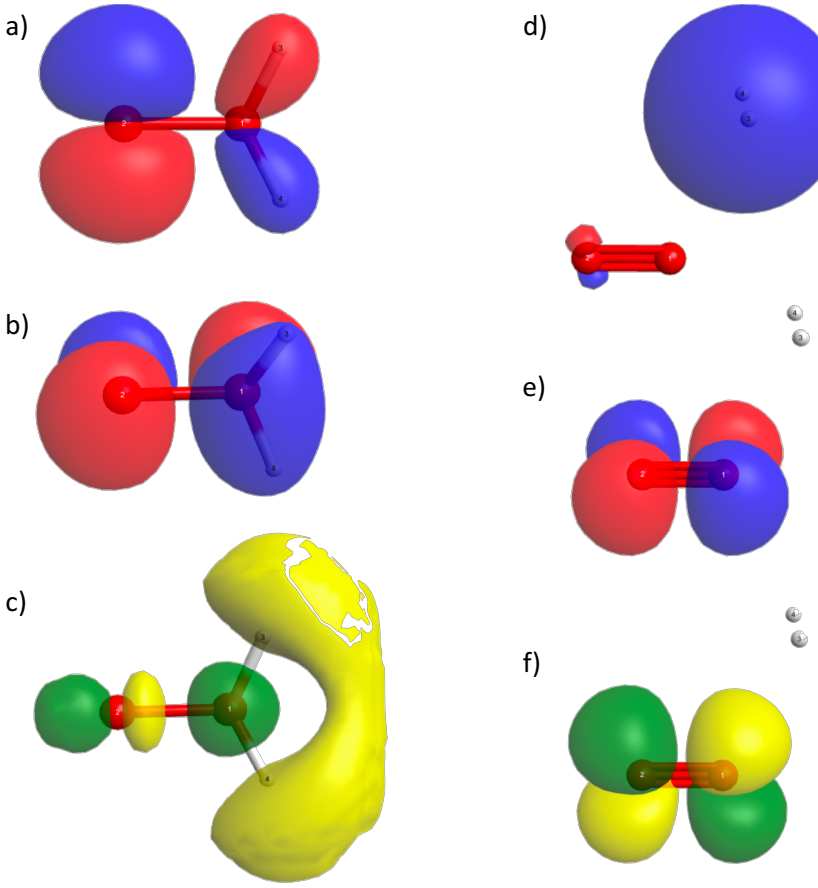

As shown in Figure 2, the electronic states of H_2OO^+ and that from the $H_2\cdots O_2{}^+$ complex have different orbital occupations, but the topologies of the orbitals themselves largely remain consistent. The ground $X\ ^2A'$ state of the oxywater cation has a $(\text{core})(3a')^2(4a')^2(1a'')^2(5a')^2(6a')^2(2a'')^2(7a')$ orbital occupation. The other doublet ($1\ ^2A''$, red line in Figure 1) excites one electron from the $2a''$ orbital into the $7a'$ as shown in Figure 3. The $1\ ^4A''$ state excites one electron from the same $2a''$ orbital in the ground $X\ ^2A'$ state of H_2OO^+ into a higher $8a'$ in the third column in Figure 3. These three orbitals in this active space represent the three antibonding p orbital combinations from the oxygens: $2a''$ being the π_y^*, $7a'$ the π_z^* highest-occupied molecular orbital (HOMO), and $8a'$ the σ^* lowest-unoccupied molecular orbital (LUMO). These are visually depicted in Figures 2a-2c, respectively.

FIG. 3. The H_2OO^+ MO Occupations for the $X\ ^2A'$, $1\ ^2A''$, and $1\ ^4A''$ States of H_2OO^+ and the $^2A''$ State of $H_2\cdots O_2{}^+$ as Labeled from the $X\ ^2A'$ State.

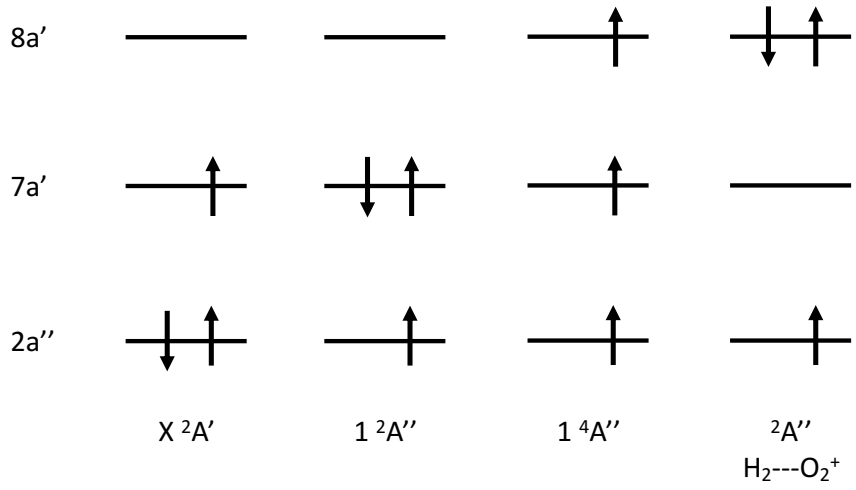

The $^2A''$ $H_2\cdots O_2{}^+$ complex occupation is defined as $(\text{core})(3a')^2(4a')^2(1a'')^2(5a')^2(6a')^2(7a')^2(2a'')$ and is compared to the other states' occupations in the last column of Figure 3. Hence, the $^2A''$ $H_2\cdots O_2{}^+$ state and the ground $X\ ^2A'$ state of H_2OO^+ have the same occupation of the same orbitals up to the HOMO-2 $6a'$ orbital. These are mostly the expected O_2 MOs for the first six levels. The actual HOMO-1, HOMO, and LUMO for this complex are all shown in Figures 2d-2f. In this complex, the $7a'$ HOMO-1 is the H−H σ bond, the $2a''$ HOMO is the π_y^*, and the $8a'$ LUMO is the π_z^*.

At first glance, these two sets of MOs appear unrelated, but a closer inspection indicates that they are actually connected as is further exposed in Figure 3. The key is from the

1 $^4A''$ state where the H_2OO^+ $8a'$ orbital is singly-occupied. As shown in Figure 2c, the hydrogen atoms are in-phase with one another even if the adjacent atoms have antibonding interactions. Similar σ antibonding but in-phase hydrogen backbonding has been previously shown in the related 1 $^4A''$ state of H_2SS^{+12}. This is the same topology as the $7a'$ HOMO-1 (H−H σ-bonding orbital) in $H_2\cdots O_2{}^+$ shown in Figure 2d. Succinctly, the difference between the MOs in H_2OO^+ and $H_2\cdots O_2{}^+$ can be described from Figure 2 where a, b, and c become e, f, and d, respectively. Hence, a spin-flip excitation in the 1 $^4A''$ H_2OO^+ state out of the $7a'$ HOMO into the $8a'$ LUMO would create orbital occupations consistent with the occupations of the $^2A''$ state of $H_2\cdots O_2{}^+$ again shown in Figure 3.

FIG. 4. The $^2A''$ $H_2\cdots O_2{}^+$ 2D PES with energy gradations in kcal/mol.

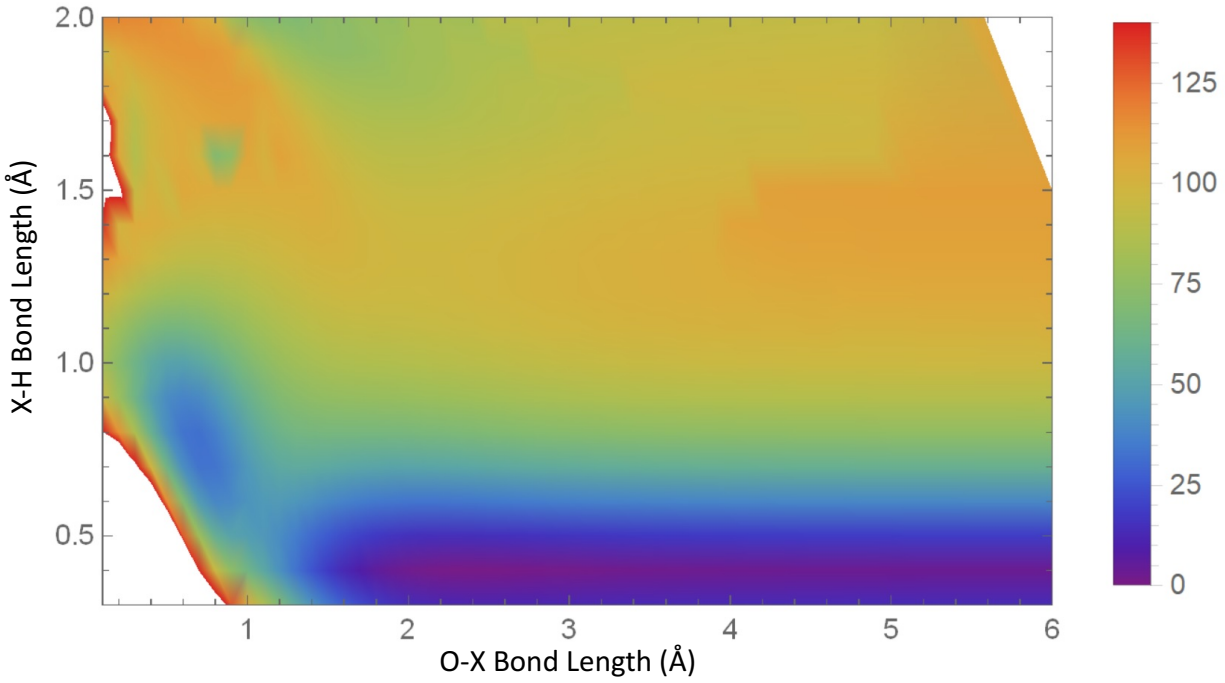

The 1 $^4A''$ state of H_2OO^+ and $^2A''$ $H_2\cdots O_2{}^+$ have further commonalities. The ∠O−O−X is close between the two at 112.9° and 111.5°, respectively, from Table I. Figure 4 is a $^2A''$ two-dimensional PES scanning over the X−H and O−X bond lengths in this case where ∠O−O−X and O−O are frozen at the optimized $^2A''$ $H_2\cdots O_2{}^+$ values. The $H_2\cdots O_2{}^+$ minimum is clearly produced, but a second local minimum 31.7 kcal/mol (1.37 eV) above the minimum for the complex is also present. The X−H value (y) is 0.8 Å, and the O−X value (x) is 0.7 Å at this local minimum in Figure 4. These values are nearly the same as the

X−H and O−X bond lengths in 1 $^4A''$ H_2OO^+ indicating that the $^2A'' \leftarrow {}^4A''$ excitation in H_2OO^+ takes place here. The excitation energy is approximated to be 44.3 kcal/mol (1.92 eV or 645 nm) in this region since, again, 1 $^4A''$ H_2OO^+ and $^2A''$ $H_2\cdots O_2{}^+$ are separated by 12.6 kcal/mol. Additionally, a saddle point between these two minima at X−H=0.6 Å and O−X=1.1 Å lies 46.0 kcal/mol (1.99 eV) above the $H_2\cdots O_2{}^+$ minimum.

Hence, the 1 $^4A''$ state of H_2OO^+ and the $^2A''$ $H_2\cdots O_2{}^+$ state could interact in the region where the blue second minimum in Figure 4 occurs. This $^2A'' \leftarrow {}^4A''$ excitation appears to take place in the red of the visible spectrum clearly within the wavelengths of sunlight. Other $H_2\cdots O_2{}^+$ minima have also been localized in this study, but their X−O bond distances are greater than 4.0 Å. In order to fully characterize any transition from the H_2OO^+ into the $H_2\cdots O_2{}^+$, spin-flip excited state determinants and electron dynamics computations originating with the 1 $^4A''$ state of H_2OO^+ or a semi-global 6D PES surface are necessary in future work. However, the local minimum described above is a very promising region to explore the formation of $O_2{}^+$ from water in the gas phase.

In conclusion, the oxywater cation is shown here to be a possible intermediate in the creation of molecular oxygen from water cations and atomic oxygen. The formation of the oxywater cation begins with O(^3P) atoms bonding with water cations to produce 1 $^4A''$ H_2OO^+. Before becoming X $^2A'$ or 1 $^2A''$ H_2OO^+, the quartet state may convert to a different $^2A''$ state, instead: $H_2\cdots O_2{}^+$. The minimum of 1 $^4A''$ H_2OO^+ and $^2A''$ $H_2\cdots O_2{}^+$ are only 12.6 kcal/mol apart adiabatically. Furthermore, the lowest 1 $^4A''$ state of H_2OO^+ has a similar geometry to the local minimum on the $^2A''$ PES corresponding to the $H_2\cdots O_2{}^+$ complex. The approximated $^2A'' \leftarrow {}^4A''$ excitation for H_2OO^+ in this region is 645 nm, and further refinements of this value likely leading to the $H_2\cdots O_2{}^+$ complex should not shift it out of the range for solar radiation. The resulting complex after excitation and crossing a low-lying saddle point is then easily dissociated into molecular hydrogen and molecular oxygen. Consequently, the oxywater cation and its $H_2\cdots O_2{}^+$ complex give all indication of facilitating the creation of molecular oxygen. This has application to various natural processes ranging from the creation of surprisingly high amounts of molecular oxygen in the coma of comet 67P/Churyumov-Gerasimenko observed during the *Rosetta* mission[13] to the provenance of oxygen on the early Earth potentially including the "snowball Earth" epoch and even to oxygen generation in the upper atmosphere where climate change is driving more water vapor into the stratosphere where it can ionize and react with known atomic

oxygen.

COMPUTATIONAL DETAILS

All relative energies and PES scans employ the CCSD(T)-F12/cc-pVTZ-F12 level of theory, except where MRCISD(+Q)/aug-cc-pVTZ is noted. In either case, the MOLPRO2015.1 quantum chemistry program[14,15] is solely utilized. All geometry optimizations are followed by harmonic vibrational frequency computations to ensure that the structures examined are minima and to provide the harmonic zero-point vibrational corrections which are included in the relative energy determinations. The PES scans have displacements of 0.1 Å for the O−O bond lengths (Figure 1), 0.2 Å for the O−X bond lengths (Figure 4), and 0.1 Å displacements for the X−H bond lengths (Figure 4).

SUPPLEMENTARY INFORMATION

The SI contains the MRCISD(+Q)/aug-cc-pVTZ data as a scan of states for the O−O bond elongation.

ACKNOWLEDGEMENTS

Support is acknowledged from NASA grant NNX17AH15G issued through the Science Mission Directorate, NSF REU grant CHE-1460568 and NSF grant OIA-1757220, and start-up funds provided by the University of Mississippi.

---

* r410@olemiss.edu

[1] B. R. Westbrook, K. M. Dreux, G. S. Tschumper, J. S. Francisco, and R. C. Fortenberry, Phys. Chem. Chem. Phys. **20**, 25967 (2018)

[2] J. M. Hollis, E. B. Churchwell, E. Herbst, and F. C. de Lucia, Nature **322**, 524 (1986)

[3] C. Meredith, T. P. Hamilton, and H. F. Schaefer III, J. Phys. Chem. **96**, 9250 (1992)

[4] Y. Xie, W. D. Allen, Y. Yamaguchi, and H. F. Schaefer III, J. Chem. Phys. **104**, 7615 (1996)

[5] J. Franz, J. S. Francisco, and S. D. Peyerimhoff, J. Chem. Phys. **130**, 084304 (2009)

[6] T. B. Adler, G. Knizia, and H.-J. Werner, J. Chem. Phys. **127**, 221106 (2007)

[7] G. Knizia, T. B. Adler, and H.-J. Werner, J. Chem. Phys. **130**, 054104 (2009)

[8] H.-J. Werner and E.-A. Reinsch, J. Chem. Phys. **76**, 3144 (1982)

[9] T. H. Dunning, J. Chem. Phys. **90**, 1007 (1989)

[10] K. P. Huber, G. Herzberg, J. W. Gallagher, and R. D. Johnson, III, in *Constants of Diatomic Molecules*, edited by P. J. Linstrom and W. G. Mallard (National Institute of Standards and Technology, Gaithersburg MD, 20899, 2018) p. 69

[11] R. C. Fortenberry and S. R. Gwaltney, ACS Earth Space Chem. **2**, 491 (2018)

[12] R. C. Fortenberry, T. Trabelsi, and J. S. Francisco, J. Phys. Chem. A **122**, 4983 (2018)

[13] A. Bieler, K. Altwegg, H. Balsiger, A. Bar-Nun, J.-J. Berthelier, P. Bochsler, C. Briois, U. Calmonte, M. Combi, J. De Keyser, E. F. van Dishoeck, B. Fiethe, S. A. Fuselier, S. Gasc, T. I. Gombosi, K. C. Hansen, M. Hässig, A. Jäckel, E. Kopp, A. Korth, L. L. Roy, U. Mall, R. Maggiolo, B. Marty, O. Mousis, T. Owen, H. Rème, M. Rubin, T. Sémon, C.-Y. Tzou, J. H. Waite, C. Walsh, and P. Wurz, Nature **526**, 678 (2015)

[14] H.-J. Werner, P. J. Knowles, G. Knizia, F. R. Manby, M. Schütz, P. Celani, W. Györffy, D. Kats, T. Korona, R. Lindh, A. Mitrushenkov, G. Rauhut, K. R. Shamasundar, T. B. Adler, R. D. Amos, A. Bernhardsson, A. Berning, D. L. Cooper, M. J. O. Deegan, A. J. Dobbyn, F. Eckert, E. Goll, C. Hampel, A. Hesselmann, G. Hetzer, T. Hrenar, G. Jansen, C. Köppl, Y. Liu, A. W. Lloyd, R. A. Mata, A. J. May, S. J. McNicholas, W. Meyer, M. E. Mura, A. Nicklass, D. P. O'Neill, P. Palmieri, D. Peng, K. Pflüger, R. Pitzer, M. Reiher, T. Shiozaki, H. Stoll, A. J. Stone, R. Tarroni, T. Thorsteinsson, and M. Wang, "Molpro, version 2015.1, a package of *ab initio* programs," (2015), see http://www.molpro.net

[15] H.-J. Werner, P. J. Knowles, G. Knizia, F. R. Manby, and M. Schütz, WIREs Comput. Mol. Sci. **2**, 242 (2012)